GMR
The Original

BIOPOLYMERIC ELECTROSPUN NANOSCAFFOLDS INCORPORATED WITH GREEN SYNTHESISED CuO NANOPARTICLES FROM RED MARINE MACROALGAE EXTRACT FOR WOUND HEALING ACTIVITY

Lishya Sri Nagaraj[1], Afrin faheema J[2], Sattanathan Govindharajan[3]*

[1]Saveetha Medical College & Hospital (SMCH), Saveetha Institute of Medical and Technical Sciences (SIMATS), Thandalam, Chennai, Tamil Nadu 602105, India. lishya2212@gmail.com
[2]Department of Dermatology, Saveetha Medical College and Hospital, Saveetha Institute of Medical And Technical Sciences (SIMATS), Thandalam, Chennai-602105, Tamil Nadu, India. Email: drafrin.derm@gmail.com
[3]Department of Pathology, Saveetha Medical College and Hospital, Saveetha Institute of Medical And Technical Sciences (SIMATS), Thandalam, Chennai-602105, Tamil Nadu, India. Email: sattanathanphd@gmail.com
*Corresponding Author: sattanathanphd@gmail.com (S.G.)

ABSTRACT
This study reports the green synthesis of copper oxide nanoparticles (CuO NPs) using *Gracilaria corticata* red algal extract via an ultrasonic-assisted method, followed by their incorporation into starch/polyvinyl alcohol (PVA) electrospun nanoscaffolds for enhanced wound healing applications. UV-Vis spectroscopy confirmed nanoparticle formation with a characteristic surface plasmon resonance (SPR) peak at 291 nm, while Fourier-transform infrared spectroscopy (FTIR) analysis revealed bioactive functional groups from algal extract acting as reducing and stabilizing agents. X-ray diffraction (XRD) confirmed the monoclinic crystalline structure of CuO NPs, whereas Scanning electron microscopy (SEM) demonstrated uniform dispersion within nanofibers without aggregation. Thermogravimetric analysis (TGA) indicated improved thermal stability (degradation onset at 265.25°C), and Dynamic light scattering (DLS) analysis showed moderate colloidal stability (zeta potential: -14.11 mV). The wound healing scratch assay on HaCaT keratinocytes revealed concentration-dependent activity, with starch/PVA/CuO-NPs nanoscaffolds exhibiting superior performance (97.59% closure at 100 µg/mL) compared to CuO NPs (85.59%) and algal extract alone (71.59%). The nanoscaffold's fibrous architecture and bioactive CuO NPs synergistically enhanced cell migration, underscoring its potential as an advanced wound dressing. This study highlights the efficacy of eco-friendly CuO NPs and their nanocomposites in accelerating tissue regeneration, offering a sustainable approach for biomedical applications.

KEYWORDS: *Gracilaria corticata*, Green synthesis, CuO nanoparticles, starch/PVA/CuO-NPs nanoscaffolds, Wound-healing activity.

1. INTRODUCTION

Wound healing is a multifaceted biological process involving a cascade of cellular and molecular events aimed at restoring the integrity and function of damaged tissue [1-4]. Impaired healing due to microbial infections, oxidative stress, or chronic conditions such as diabetes can delay recovery and result in significant healthcare challenges [5-9]. The demand for effective, biocompatible wound dressings that accelerate healing while minimizing infection has fueled extensive research into advanced biomaterials and therapeutic scaffolds [10]. Electrospun nanofibrous scaffolds, in particular, have emerged as promising candidates due to their structural similarity to the native extracellular matrix (ECM), high surface area-to-volume ratio, and potential for controlled drug or nanoparticle incorporation [11, 12].

Natural polymers such as starch and synthetic counterparts like polyvinyl alcohol (PVA) are frequently employed in biomedical scaffold fabrication owing to their biocompatibility, biodegradability, and mechanical flexibility [13]. Starch, a polysaccharide derived from various plant sources, offers excellent moisture retention, low toxicity, and renewability [14-16]. However, its native mechanical properties and electrospinnability are often suboptimal [17]. To overcome these limitations, it is frequently blended with PVA, which enhances the mechanical integrity and facilitates nanofiber formation through electrospinning [18]. This hybrid polymer system provides a versatile platform for the incorporation of therapeutic agents, including metal oxide nanoparticles, to endow additional functionality such as antimicrobial activity and oxidative stress mitigation [19, 20].

Among metal oxide, copper oxide nanoparticles (CuO NPs) stands out due to its excellent antimicrobial, antioxidant, and pro-angiogenic properties, all of which are vital for accelerating wound repair [21]. Copper plays a key role in several physiological processes such as angiogenesis, collagen synthesis, and tissue regeneration [22]. Incorporation of CuO NPs into polymeric scaffolds has shown significant potential in enhancing wound healing efficacy [23]. However, conventional chemical synthesis methods of CuO NPs often involve hazardous reagents and generate toxic byproducts, limiting their biomedical applicability [24, 25]. To address these issues,

green synthesis routes utilizing biological systems such as plant extracts, fungi, or algae have gained momentum due to their eco-friendly, cost-effective, and biocompatible nature [26, 27].
Marine macroalgae, particularly *Gracilaria corticata*, are rich in polysaccharides, polyphenols, flavonoids, and other phytochemicals that can serve as natural reducing and stabilizing agents in the green synthesis of nanoparticles [28]. This red seaweed, abundantly found in coastal regions of South India, has been traditionally used in food, agriculture, and medicine [29]. Recent studies have revealed its potential in bioremediation and nanobiotechnology due to its phytochemical-rich profile [30, 31]. When combined with green synthesis techniques such as ultrasonic-assisted extraction (UAE), which enhances cell wall disruption and extraction efficiency, *G. corticata* serves as an ideal candidate for the biosynthesis of functional metal oxide nanoparticles [32]. UAE further reduces energy consumption and processing time while preserving thermolabile bioactives, making it suitable for biomedical nanoparticle preparation [33, 34].
In this context, the present study explores the development of a novel nanofibrous wound dressing scaffold by integrating CuO NPs synthesized via ultrasonic-assisted green synthesis using *G. corticata* extract into a starch/PVA electrospun matrix [35, 36]. The hybrid scaffold aims to combine the physicochemical robustness of the polymer blend with the biological functionality of CuO NPs to create a multifunctional platform for enhanced wound management [37]. The green synthesis strategy not only ensures the ecological safety of the CuO NPs but also leverages the intrinsic bioactivity of marine-derived phytochemicals [38].
The synthesized nanoparticles and the fabricated nanoscaffolds were subjected to comprehensive physicochemical characterization which provided insights into particle size, structural integrity, functional groups, surface charge, crystalline nature, and thermal stability—factors critical to their biomedical application [39]. To assess the therapeutic potential of the developed scaffolds, an *in vitro* scratch wound assay using HaCaT human keratinocyte cells was conducted [40]. The assay aimed to evaluate the cell migration and proliferation behavior in the presence of the algal extract, green-synthesized CuO NPs, and CuO-loaded nanofiber scaffolds [41-44]. Cell migration is a vital step in wound closure and re-epithelialization, and materials that enhance this process are considered advantageous for wound healing applications [45].
The novelty of this study lies in its integrative approach, combining ultrasonic-assisted extraction, marine-based green synthesis of metal oxide nanoparticles, and electrospun nanofiber technology for wound healing applications. Unlike previous studies that focus on either green synthesis or scaffold fabrication in isolation, this research bridges the two domains to develop a sustainable and bioactive wound dressing material. Furthermore, the use of *G. corticata*, an underexplored marine alga, adds a new dimension to the field of algal nanobiotechnology.

2. MATERIALS AND METHODS

2.1 Chemicals and reagents

The marine brown alga *G. corticata* was collected from the Rameswaram coastline, Tamil Nadu, India, and utilized as a sustainable and eco-friendly reducing agent for the biosynthesis of CuO NPs. Analytical-grade copper(II) sulfate pentahydrate ($CuSO_4 \cdot 5H_2O$) from Merck served as the copper source. PVA, with an approximate molecular mass of 115,000 g/mol, along with starch, was selected to create biocompatible nanofiber matrices. Nanofiber fabrication was carried out using a HOLMARC HO-NFES-040 electrospinning unit. All chemicals and solvents used, sourced from Sigma-Aldrich and Merck, met analytical-grade standards to ensure consistent and reproducible experimental outcomes. Characterization of CuO NPs and scaffold materials included UV-Vis spectroscopy, Fourier-transform infrared spectroscopy (FTIR), X-ray diffraction (XRD), Scanning electron microscopy (SEM), Dynamic light scattering (DLS), zeta potential analysis, and Thermogravimetric analysis (TGA). HaCaT keratinocytes cells were obtained from the National Centre for Cell Science (NCCS), Pune, India, which provided authenticated and contamination-free cell stocks for biological investigations focused on assays were used to determine the wound healing activity of the developed scaffolds.

2.2 Collection and processing of marine algae

Specimens of *G. corticata*, a brown macroalga, were gathered from intertidal regions along the coast of Rameswaram. The collected *Gracilaria corticate* was taxonomically identified and authenticated by Dr V. Veeragurunathan, CSIR-CSMCRI-Marine Algal Research Station, Mandapam Camp 623519, Tamil Nadu, India. A voucher specimen was prepared and deposited at the Herbarium of the CSIR-CSMCRI-Marine Algal Research Station, under the accession number: SI–2025–RMM–019. This authentication ensures botanical accuracy and standardization of the study material. Immediately after collection, samples were stored in iceboxes to retain their bioactive integrity. The seaweed was thoroughly washed with tap water to remove adhered impurities and rinsed repeatedly with distilled water to eliminate residual salts. A quantity of 100 g of cleaned algae was chopped into small sections and dried at ambient temperature for 14 days. The completely dried biomass was then ground into a fine powder using a mechanical grinder and stored in airtight containers under cool and moisture-free conditions until further use in extraction procedures.

2.3 Ultrasonic-Assisted Extraction of bioactive compounds

To enhance cell wall disruption and extraction efficiency, bioactive components were isolated from *G. corticata* powder using ultrasonic-assisted extraction (UAE). Two grams of the dried algae powder were mixed with 50 mL Milli-Q water in a 100 mL borosilicate glass container. This mixture underwent sonication at 60°C for 45 minutes

using a LABQUEST ultrasonic cleaner (Borosil; Serial No. 941032329018). The resulting solution was filtered using sterile Whatman No. 1 filter paper to obtain a clear extract, which was subsequently stored at 10°C. A portion of this filtrate was freeze-dried and reserved for the biosynthesis of CuO NPs [46, 47].

2.4 Green synthesis of CuO NPs

The CuO NPs were synthesized by reacting the algal extract with a copper salt solution. Specifically, 50 mL of 0.1 M $CuSO_4 \cdot 5H_2O$ aqueous solution was mixed with 10 mL of algal extract (concentration: 10 mg/mL), maintaining a volume ratio of 5:1. The reaction mixture was stirred magnetically at 650 rpm and maintained at 60°C for 2 hours. A distinct color transition from dark blue to bluish-green indicated successful phytochemical-mediated reduction of Cu^{2+} ions. The resulting CuO NPs were rinsed three times with deionized water and lyophilized for 48 hours. The obtained powder was subsequently used for scaffold incorporation and biological evaluations [48, 49].

2.5 Fabrication of starch/PVA nanofibrous scaffolds containing CuO NPs

Nanofibrous scaffolds were developed using an electrospinning approach with a polymeric blend of PVA and starch, incorporating CuO NPs. A 15% (w/w) solution of PVA was prepared by dissolving the polymer in Milli-Q water at 50°C under constant stirring. Then, 100 mg of starch and 100 mg of synthesized CuO NPs were added and stirred at 50°C for 2.5 hours to ensure uniform dispersion. This homogeneous viscous solution was loaded into a 10 mL syringe fitted with a stainless-steel needle (inner diameter: 0.84 mm). Electrospinning was conducted using a HOLMARC HO-NFES-040 machine under the following settings: applied voltage of 11.5 kV, tip-to-collector distance of 12.3 cm, and a flow rate of 0.4 mL/h. The process lasted for 6 to 8 hours at room temperature. The resulting nanofiber mats were collected and stored in desiccators to preserve their structure [50-53].

2.6 Physicochemical characterization

2.6.1 UV-visible spectroscopy

UV-Vis spectral analyses were carried out for the algal extract, synthesized CuO NPs, and CuO-loaded nanofiber scaffolds using a VIS SPEC V-730 spectrophotometer. Spectra were recorded between 200–800 nm, using deionized water as the baseline. Absorption bands observed between 270–300 nm confirmed the surface plasmon resonance of CuO NPs, indicating successful formation [54, 55].

2.6.2 FTIR spectroscopy

Functional group characterization was conducted via FTIR using a PerkinElmer Spectrum Two instrument in ATR mode. Spectral data were collected in the range of 4000–400 cm^{-1} at 4 cm^{-1} resolution over 64 scans. Bands related to hydroxyl (O–H), carbonyl (C=O), amide, and Cu–O vibrations were indicative of the successful embedding of nanoparticles within the polymer matrix [56, 57].

2.6.3 XRD analysis

XRD analysis was performed using a Bruker D8 Advance diffractometer with CuKα radiation (λ = 1.5406 Å), operated at 40 kV and 40 mA. Scans were performed across 2θ angles from 5° to 90°, with a step increment of 0.029649°. Distinct diffraction peaks corresponding to monoclinic CuO structures verified the crystalline nature of the NPs, while altered peak positions in the composite scaffolds suggested successful nanoparticle incorporation [58].

2.6.4 SEM analysis

Surface morphology and particle dispersion within nanofibers were visualized using a JEOL JSM-IT800 NANO SEM. Prior to imaging, samples were sputter-coated with a thin layer of gold. SEM images revealed continuous nanofibers with minimal bead formation and a uniform distribution of CuO NPs across the scaffold [59].

2.6.5 TGA

Thermal behavior of the samples was assessed using a PerkinElmer TGA 8000 system. Around 5 mg of sample was heated from ambient temperature to 550°C at a rate of 15°C/min under a nitrogen stream. The thermograms exhibited stages of mass loss linked to moisture release, polymer degradation, and composite breakdown. Notably, CuO-incorporated scaffolds showed higher thermal stability than pure polymer matrices [60].

2.6.6 DLS and Zeta potential

Particle size distribution and zeta potential of CuO NPs were measured using a Malvern Zetasizer Ultra. DLS provided insights into hydrodynamic diameter and PDI, whereas zeta potential indicated colloidal stability. Nanoparticles demonstrating zeta values beyond ±30 mV were considered electrostatically stable, supporting their use in biomedical applications [61]. All datasets and results are publicly accessible through the Mendeley Data repository.

2.7 Wound healing (scratch) assay

The migratory response of HaCaT human keratinocytes was assessed using a scratch assay following treatment with algal extract, CuO NPs (NPs), and starch/PVA scaffolds loaded with CuO NPs. Cells were plated in 12-well culture plates at a density of 2×10^5 cells per well, maintained in DMEM supplemented with 10% fetal bovine serum (FBS) and 1% penicillin-streptomycin. Upon achieving confluency, a linear scratch was introduced in each well using a sterile pipette tip (200 µL). After washing with PBS to eliminate detached cells, test compounds were administered at varying concentrations (6.25, 12.5, 25, 50, and 100 µg/mL) in serum-free DMEM, while control wells remained untreated. Cell migration was monitored at 0, 24, and 48-hour intervals using an inverted phase-

contrast microscope. The extent of wound closure was quantified via ImageJ software, enabling a comparative assessment of treatment effectiveness [62].

2.8 Statistical analysis

Data analysis was conducted using SPSS (v25.0) and GraphPad Prism (v9.0). Experiments were performed in triplicate, with results presented as mean ± standard deviation. Intergroup comparisons were made using one-way ANOVA, followed by Tukey's or Dunnett's post-hoc tests as appropriate. Statistical significance was set at *p* < 0.05. Normality was verified using the Shapiro-Wilk test, with logarithmic transformation applied to non-normal datasets. Pearson's correlation coefficient was computed to examine variable relationships. All analyses were conducted within a 95% confidence interval to ensure robust interpretation [63].

3. RESULTS

3.1. UV–visible spectroscopy

The UV–Visible spectral analysis (Figure 1) elucidated the optical properties of both the *G. corticata* extract and the biosynthesized CuO NPs. The aqueous extract displayed a broad absorption spectrum ranging from 200 nm to 800 nm, with a notable peak at 302 nm and an absorbance value of 1.268. This broad absorption is characteristic of phytochemicals such as polyphenols and flavonoids, which play a crucial role in reducing and stabilizing metal ions during nanoparticle formation. In contrast, the CuO NPs exhibited a distinct surface plasmon resonance (SPR) peak centered at 291 nm, indicative of nanoparticle formation due to the collective oscillation of conduction electrons. Additionally, the CuO NPs showed significant absorbance near 800 nm (1.200), which gradually decreased towards shorter wavelengths, aligning with the typical behavior of metal oxide nanoparticles. The absence of sharp features in the extract and the presence of a clear SPR peak in the nanoparticle sample confirm the successful biosynthesis of CuO NPs mediated by the G. corticata extract, serving as a natural reducing and capping agent.

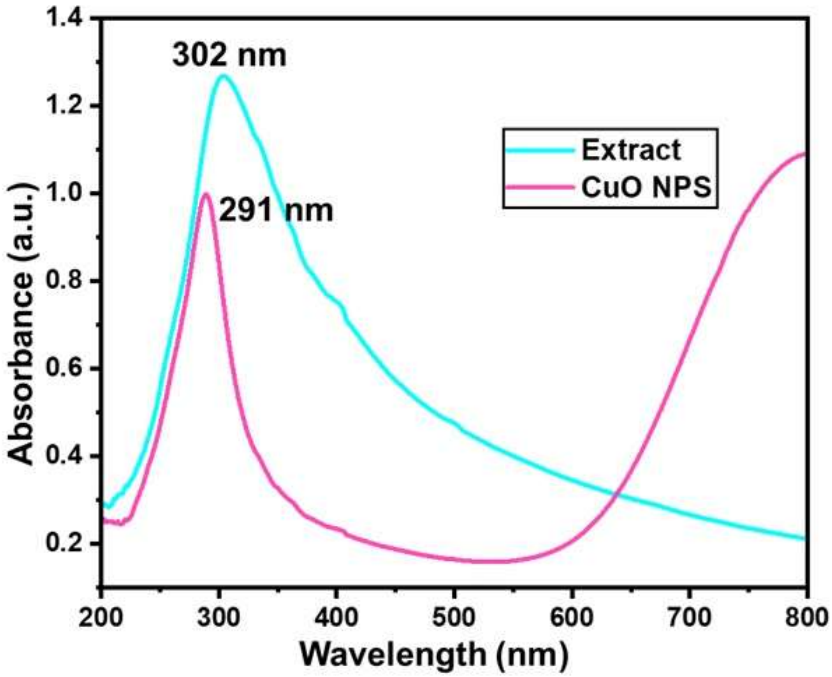

Fig. 1. UV–Visible spectral profiles of algal extract and CuO NPs.

3.2. FTIR spectroscopy analysis

FTIR spectroscopy (Figure 2) was employed to identify the functional groups present in the CuO NPs and the nanoscaffold composite. The spectrum of CuO NPs revealed prominent absorption bands corresponding to O–H stretching vibrations and Cu–O bonds, confirming the formation of metal–oxygen linkages. The nanoscaffold spectrum exhibited ten characteristic peaks, including a broad O–H stretch at 3303.50 cm^{-1}, a carbonyl C=O stretch at 1709.35 cm^{-1}, and aliphatic C–H stretching at 2924.80 cm^{-1}. Additional peaks at 1427.14, 1329.09, 1141.87, 1088.65, 919.75, 843.06, and 601.37 cm^{-1} were indicative of polymeric constituents such as amides and polysaccharides. These spectral features demonstrate the successful incorporation of CuO NPs into the polymer matrix, with interactions likely facilitated by metal coordination and hydrogen bonding. The presence of bioactive groups derived from *G. corticata* suggests its role in stabilizing the nanoparticles at the interface.

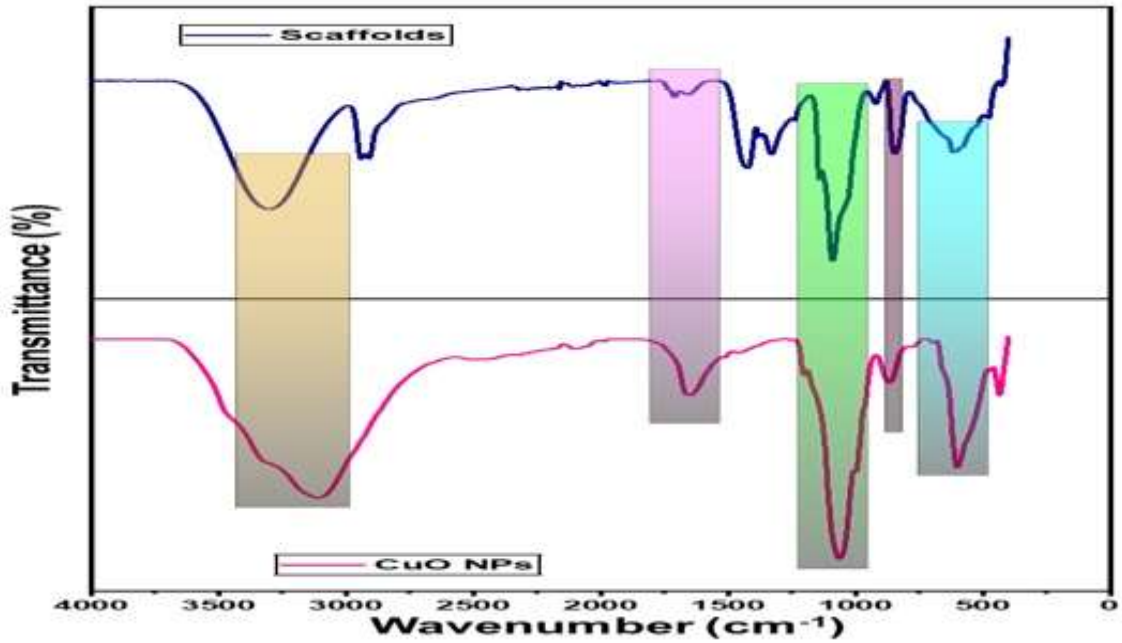

Fig. 2. FTIR spectra of CuO NPs and their incorporation into nanoscaffolds.

3.3. XRD analysis

XRD analysis (Figure 3) was conducted to determine the crystalline nature of the synthesized CuO NPs and the nanoscaffold composite. The CuO NPs displayed 37 diffraction peaks within the 2θ range of 12.852° to 57.284°, with intense reflections at 19.134°, 24.369°, and 15.797°, corresponding to monoclinic CuO as per JCPDS card 48-1548. These reflections correspond to d-spacing values of 4.63468 Å, 3.64963 Å, and 5.60549 Å, confirming the crystalline purity of the nanoparticles. The nanoscaffold exhibited 13 diffraction peaks, notably at 29.445° and 21.346°, indicative of a semi-crystalline architecture composed of approximately 20.2% crystalline and 79.8% amorphous phases. Broadened peaks, such as the one at 43.067° with a full width at half maximum (FWHM) of 1.025°, suggested small crystallite sizes and effective dispersion of CuO NPs within the polymer. Minor peak shifts, like from 35.999° to 36.034°, implied strong interfacial bonding likely mediated by phytochemicals from the *G. corticata* extract, enhancing nanoparticle–polymer interactions.

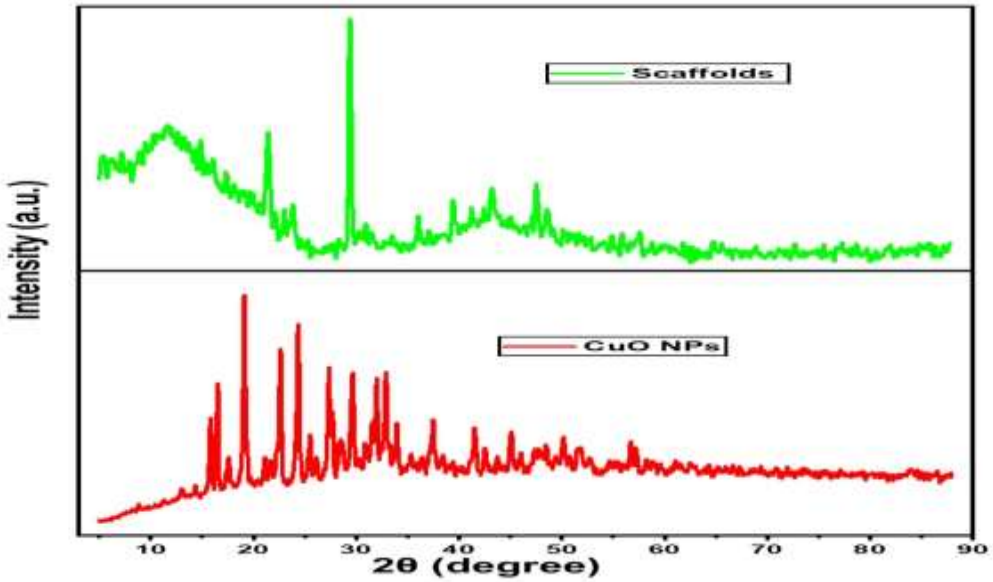

Fig. 3. XRD patterns of synthesized CuO NPs and CuO-loaded scaffolds.

3.4. SEM analysis

SEM analysis (Figure 4) was utilized to examine the morphology of CuO NPs embedded within electrospun starch/PVA nanoscaffolds. Micrographs revealed a continuous network of fibers with smooth surfaces, measuring between 90 and 150 nm in diameter. The absence of beads or defects indicated successful electrospinning. Spherical CuO NPs, smaller than 100 nm, were homogeneously distributed across the fiber surfaces and embedded within the scaffold without aggregation. This uniform dispersion confirms effective mixing of nanoparticles with the polymer solution prior to electrospinning. The preserved fibrous morphology confirms compatibility between

CuO NPs and the starch/PVA matrix. The bioactive compounds in *G. corticata* extract likely contributed to nanoparticle stabilization and prevented agglomeration through natural capping effects.

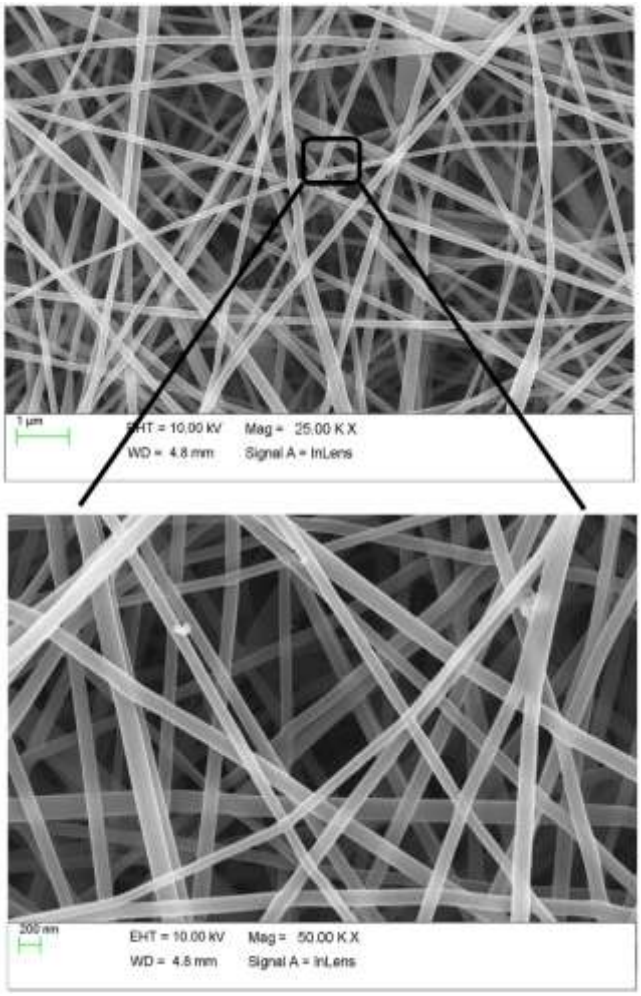

Fig. 4. SEM analysis of synthesized CuO NPs **and CuO-loaded scaffolds.**

3.5. TGA

TGA (Figure 5) was performed to assess the thermal stability of the nanoscaffold. The analysis involved heating the sample from 30°C to 550°C at a rate of 15°C/min. The resulting thermogram revealed two principal degradation phases: the first initiating at 265.25°C and peaking at 355.41°C, attributed to the decomposition of organic residues and polymer components; the second phase starting at 425.38°C with a maximum degradation temperature of 448.38°C, associated with the breakdown of more thermally stable constituents. The total mass loss was 33.372%, illustrating the scaffold's thermal decomposition profile. The relatively high onset of degradation suggests enhanced thermal stability, likely due to CuO NP reinforcement and potential cross-linking within the polymer. Furthermore, secondary metabolites from *G. corticata* may contribute to improved thermal properties by interacting protectively with polymer chains.

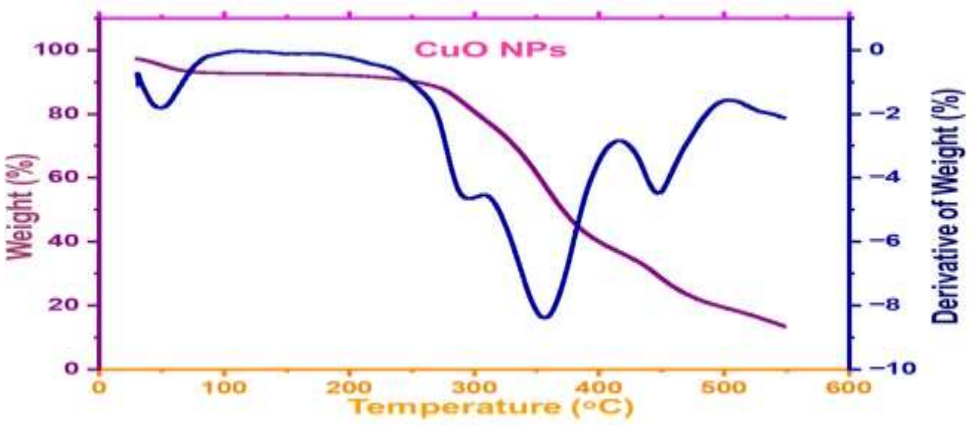

Fig. 5. Thermal degradation behavior of CuO-incorporated nanoscaffolds.

3.6. DLS and Zeta Potential Analysis

DLS and zeta potential measurements were conducted to characterize the colloidal behavior of the biosynthesized CuO NPs. The nanoparticles exhibited a bimodal size distribution with an average hydrodynamic diameter (Z-average) of 68.6 nm (Figure 6) and a polydispersity index (PDI) of 0.584, indicating moderate size heterogeneity. The zeta potential was recorded at -14.11 mV, with distribution peaks at -25.21 mV and -5.514 mV (Figure 7), reflecting a moderately negative surface charge which confers partial colloidal stability. This negative charge is attributed to the biomolecules from the *G. corticata* extract adsorbed on the nanoparticle surface. Conductivity was measured at 0.05175 mS/cm, and the wall zeta potential registered -12.73 mV. While the observed values suggest reasonable dispersion stability, further surface modification may be necessary to optimize long-term stability, especially for biomedical applications that demand consistent nanoparticle behavior.

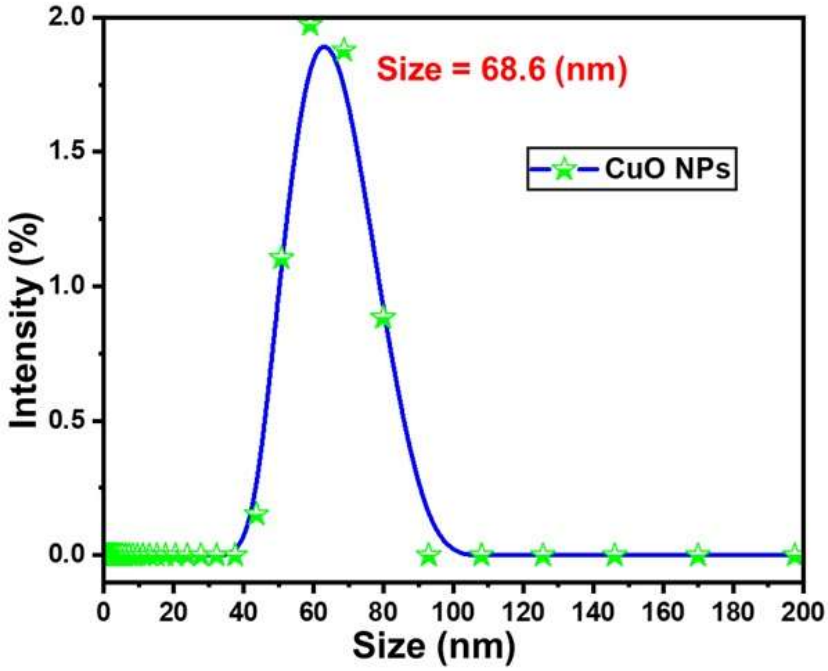

Fig.6. DLS particles size analysis of CuO NPs

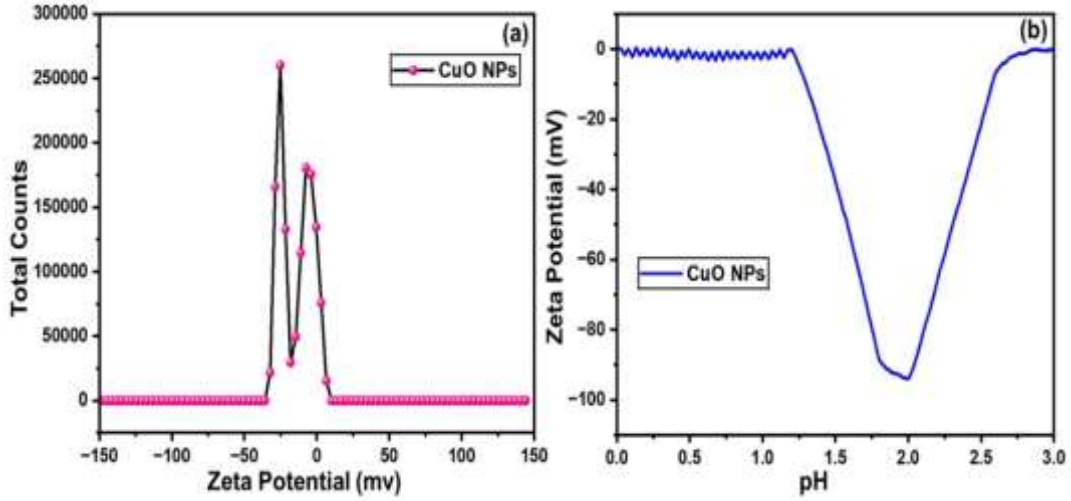

Fig.7. Zeta-potential analysis of CuO NPs

3.7. Wound Healing (Scratch) Assay

The wound healing (scratch) assay (Fig. 8) demonstrated significant differences in the migratory behavior of HaCaT keratinocyte cells after 48 hours of treatment with algal extract, CuO NPs, and starch/PVA/CuO-NPs nanoscaffolds. At the lowest concentration (6.25 µg/mL), the algal extract exhibited a wound closure rate of 34.59%, while CuO NPs and nanoscaffolds showed higher closure rates of 42.59% and 49.59%, respectively. As the concentration increased to 12.5 µg/mL, the algal extract promoted 41.59% wound closure, whereas CuO NPs and nanoscaffolds further enhanced migration, achieving 48.59% and 64.59% closure, respectively.

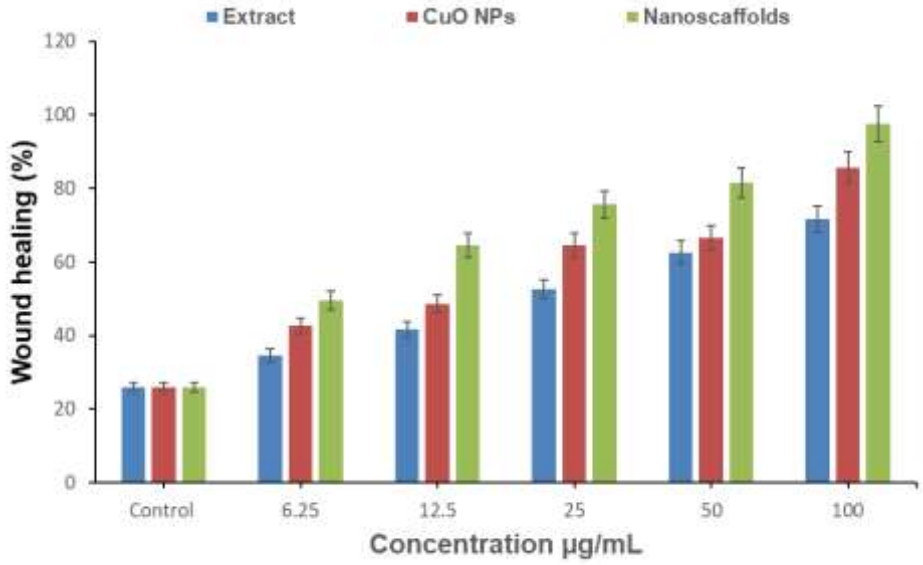

Fig. 8. Wound healing activity of algal extract, CuO NPs and starch/PVA/CuO-NPs nanoscaffolds

At 25 µg/mL, the algal extract facilitated 52.59% wound closure, while CuO NPs and nanoscaffolds demonstrated more pronounced effects, with closure rates of 64.59% and 75.59%, respectively. The trend continued at higher concentrations: at 50 µg/mL, the algal extract reached 62.59% closure, compared to 66.59% for CuO NPs and 81.59% for nanoscaffolds. The highest concentration (100 µg/mL) revealed the most striking results, with the algal extract achieving 71.59% wound closure, CuO NPs reaching 85.59%, and nanoscaffolds exhibiting the highest efficacy at 97.59%.

These results indicate that all three treatments enhanced wound healing in a concentration-dependent manner. However, the starch/PVA/CuO-NPs nanoscaffolds consistently outperformed both the algal extract and CuO NPs alone, suggesting superior cell migration-promoting properties. The improved performance of the nanoscaffolds may be attributed to their composite structure, which likely provides a more favorable microenvironment for cell proliferation and migration. The findings highlight the potential of these nanoscaffolds as a promising therapeutic option for accelerating wound healing.

4. DISCUSSION

The research presents a comprehensive investigation into the development and evaluation of starch/PVA-based electrospun nanoscaffolds incorporated with green-synthesized CuO NPs, derived from *G. corticata* extract. This multi-faceted study integrates physicochemical characterization and biological assessment, particularly focusing on wound healing efficacy, to explore the potential of these bioengineered nanomaterials for biomedical applications.

The initial UV–Visible spectroscopy analysis provided critical insights into the optical behavior and successful biosynthesis of CuO NPs. The distinct absorption peak at 291 nm observed in the CuO NPs, corresponding to surface plasmon resonance (SPR), confirmed the presence of metallic nanoparticles, while the broad spectrum of the *G. corticata* extract highlighted the presence of phytoconstituents such as polyphenols and flavonoids. These phytochemicals not only facilitated the reduction of copper ions but also acted as stabilizing agents, preventing aggregation and enhancing nanoparticle formation. The substantial absorbance at 800 nm further suggested the characteristic absorption profile of metal oxide NPs. Thus, the UV–Vis data substantiated the effective use of algal extract as a bio-reducing and capping agent, supporting the green synthesis approach [64].

FTIR spectroscopy was employed to identify the functional groups responsible for the stabilization and integration of CuO NPs within the polymeric matrix. The CuO NP spectra displayed peaks associated with hydroxyl (O–H) and metal–oxygen (Cu–O) bonds, reinforcing the formation of metal oxide structures. Meanwhile, the FTIR spectrum of the nanoscaffold showed prominent peaks corresponding to O–H, C=O, and C–H functional groups, alongside signals indicative of amides and polysaccharides. The coexistence of these groups demonstrated the successful incorporation of CuO NPs into the starch/PVA scaffold. The hydrogen bonding and potential coordination between the CuO NPs and polymeric chains facilitated the stable embedding of nanoparticles, a crucial feature for sustained release and functionality in wound healing applications [65, 66].

The crystalline characteristics of the synthesized nanoparticles and nanocomposites were elucidated using XRD analysis. The CuO NPs exhibited intense and sharp peaks matching the monoclinic crystalline structure of copper oxide, with diffraction angles aligning with standard JCPDS data. These peaks confirmed the high crystallinity and purity of the biosynthesized nanoparticles. The nanoscaffold composite, on the other hand, exhibited a semi-crystalline nature with broadened peaks, suggesting small crystallite sizes and effective dispersion of CuO NPs within the polymer network. Slight shifts in peak positions indicated strong interfacial interactions, likely due to

the presence of bioactive compounds from the algal extract. This crystalline-amorphous hybrid structure is advantageous in biomedical scaffolds, as it supports mechanical flexibility while enabling controlled bioactive delivery [67].

Morphological characterization through SEM revealed a uniform network of electrospun fibers with diameters ranging from 90 to 150 nm. The absence of bead formation confirmed the optimization of electrospinning parameters. Embedded CuO NPs appeared as well-dispersed spherical entities with sizes below 100 nm, indicating successful integration into the nanofiber matrix. The homogeneous distribution and lack of agglomeration are attributed to the stabilizing role of phytochemicals, which served as natural capping agents. This well-defined fibrous architecture ensures efficient cellular interaction and mimics the extracellular matrix (ECM), which is vital for tissue regeneration and wound healing [68, 69].

TGA evaluated the thermal degradation profile of the nanoscaffolds, revealing two significant weight-loss stages. The first degradation phase, occurring between 265°C and 355°C, was associated with the breakdown of organic matter and polymers, while the second phase, above 425°C, corresponded to the decomposition of more thermally stable constituents. The high degradation onset temperature and moderate mass loss (33.37%) suggest that the inclusion of CuO NPs enhanced the thermal stability of the nanocomposite. This thermal reinforcement is likely due to the interaction between nanoparticles and polymer chains, potentially strengthened by the cross-linking effect of secondary metabolites from *G. corticata* [70, 71].

DLS and zeta potential analyses offered a detailed assessment of the colloidal stability and particle size distribution. The hydrodynamic diameter of the CuO NPs averaged 68.6 nm, with a polydispersity index (PDI) of 0.584, indicating moderate size variation. The zeta potential of -14.11 mV reflected a moderately negative surface charge, which contributes to the repulsive forces necessary for colloidal stability. The surface charge originates from bioorganic residues from the algal extract adsorbed onto the nanoparticle surface. While the values denote acceptable dispersion stability, enhancements via surface modification could further improve shelf-life and consistency in biomedical settings [72, 73].

Finally, the wound healing potential was validated using an *in vitro* scratch assay. All treatment groups—*G. corticata* extract, CuO NPs, and starch/PVA/CuO-NP nanoscaffolds—exhibited dose-dependent wound closure enhancement. However, the nanoscaffolds consistently demonstrated superior efficacy, with nearly complete closure (97.59%) observed at the highest concentration (100 µg/mL). This enhanced cell migration and proliferation suggest that the composite scaffold provides a conducive microenvironment for tissue regeneration, surpassing the effects of individual components. The synergistic effects of structural integrity, sustained CuO release, and bioactive compounds culminated in the scaffold's pronounced therapeutic potential [74].

Finally, this study successfully integrates green chemistry, nanotechnology, and biomaterial engineering to develop an effective wound healing platform. The starch/PVA/CuO-NP nanoscaffolds synthesized using *G. corticata* not only demonstrated desirable physicochemical attributes but also exhibited promising biological activity. This eco-friendly, multifunctional scaffold holds significant potential for clinical translation in advanced wound management systems.

5. CONCLUSION

This study successfully demonstrated the ultrasonic-assisted green synthesis of CuO nanoparticles using *G. corticata* extract and their incorporation into starch/PVA electrospun nanoscaffolds for enhanced wound healing. Spectroscopic and microscopic analyses confirmed the formation of stable, crystalline CuO NPs with uniform dispersion in nanofibers, while FTIR and XRD revealed bioactive phytochemicals contributing to nanoparticle stabilization. The nanoscaffolds exhibited improved thermal stability and a favorable fibrous structure for cell adhesion and migration. *In vitro* wound healing assays on HaCaT cells highlighted the superior efficacy of starch/PVA/CuO-NPs nanoscaffolds, achieving 97.59% wound closure at 100 µg/mL—significantly higher than CuO NPs (85.59%) or algal extract alone (71.59%). The enhanced performance is attributed to the synergistic effects of the nanofibrous matrix and bioactive CuO NPs, which promote keratinocyte migration and tissue regeneration. These findings underscore the potential of eco-friendly, algae-mediated CuO NPs and their nanocomposites as advanced wound dressings. Future studies should explore *in vivo* applications and long-term biocompatibility to validate their clinical potential for chronic wound management.

Ethics declaration: Not Applicable

Funding Declaration: Not available for this study

Conflicts of Interest: The authors declare no conflicts of interest.

Data Availability Statement: The full dataset of physiochemical characterization associated with this work is published in Mendeley Data [Dataset] Sustainable nanohybrid systems: Physiochemical properties of *Gracilaria corticota* extract-mediated copper oxide nanoparticle-loaded starch scaffolds (DOI: 10.17632/763h4wwkrj.1).

Disclosure: The material characterization data and figures (e.g., UV, SEM, FTIR, XRD, TGA, Zeta Potential and particle sizer) presented here were generated from a common dataset and are being reused across multiple related studies on nanomaterials. All biological analyses and conclusions are original to each manuscript.

REFERENCES

[1] Dugganaboyana GK, Kannankumar MKG, Shivaramakrishna S, Raju MV, Chandrasekaran MK, Ahalliya RM, Panneerselvam N, Palanisamy CP, Kanniappan GV. Phytochemical insights, antioxidant activity and therapeutic potential of Cassia senna against prostate cancer in Wistar albino rats. Discover Applied Sciences. 2025; 7:1206.

[2] Natarajan SR, Krishnamoorthy R, Alshuniaber MA, Gatasheh MK, Rajagopal P, Veeraraghavan VP, Palanisamy CP, Jayaraman S. KDM1A Facilitates Oncogenic Potential in Colorectal Cancer Progression Through the Activation of AXIN/GSK3β/β-Catenin Signaling Pathways: Evidence From Integrated Transcriptomics and In Vitro Studies. The Journal of Gene Medicine. 2025; 27(11): e70053.

[3] Guan T, Gong J, Lin J, Palanisamy CP, Jinjin Pei J, El-Aty AMA. Machine learning-driven multimodal optimization of selenium biotransformation and flavor profiling in fermented apple–Yacon functional beverages. Innovative Food Science & Emerging Technologies. 2025; 105: 104198.

[4] Natarajan SR, Krishnamoorthy R, Alshuniaber MA, Alsulami TS, Gatasheh MK, Rajagopal P, Palanisamy CP, Govindan R, Veeraraghavan VP, Jayaraman S. ABCE1 facilitates tumour progression via aerobic glycolysis and inhibits cell death in human colorectal cancer cells through the p53 signalling pathway. Scientific Reports. 2025; 15: 24674.

[5] Huang Y, Guo H, Liu Y, Jin W, Palanisamy CP, Pei J, Oz F, El-Aty AMA. Effects of Natural Polysaccharides on the Gut Microbiota Related to Human Metabolic Health. Molecular Nutrition & Food Research. 2025; 69:e202400792.

[6] Poornima K, Meenakshi K.C, Manikandan V.R, Shankari G, Prabhu D, Rathi M.A, Palanisamy CP, Balaji R, Gopalakrishnan V.K. Exploring the anticancer potential of Jerantinine A from *Tabernaemontana coronaria* against prostate, breast, and ovarian cancers: A computational approach. *Journal of Complementary and Integrative Medicine*, 2025 22(2): 363–372.

[7] Palanisamy CP, Poompradub S, Sansanaphongpricha K, Jayaraman S, Subramani K. Faridah Sonsudin gGreen synthesis of Nigella sativa-mediated silver nanoparticles for enhanced antibacterial activity and wound healing: Mechanistic insights and biomedical applications. Environmental Nanotechnology, Monitoring & Management. 2025; 24: 101085.

[8] Surendran N, Raju MV, Chandrasekaran MK, Ahalliya RM, Palanisamy CP, Chandrasekaran G, Kanniappan GV. Physicochemical characterization of starch from Maranta arundinacea L.(arrowroot) rhizomes and its inhibition of COX-2: In vivo validation. Bioactive Carbohydrates and Dietary Fibre. 2025; 33: 100465.

[9] Kannappan P, Chandrasekaran MK, Raju MV, Gopalakrishnan S, Dhamodharan P, Ahalliya RM, Palanisamy CP, Raju B, Kanniappan GV. Exploring the anticancer potential of Jerantinine A from Tabernaemontana coronaria against prostate, breast, and ovarian cancers: a computational approach. Journal of Complementary and Integrative Medicine. 2025; 22(02): 363-372.

[10] Pei J, Kumarasamy RV, Jayaraman S, Kanniappan GV, Long Q, Palanisamy CP. Quercetin-functionalized nanomaterials: Innovative therapeutic avenues for Alzheimer's disease management. Ageing Research Reviews. 2025; 104: 102665.

[11] Natarajan PM, Umapathy VR, Murali A, Swamikannu B. (2022). Computational Simulations of Identified marine-derived Natural Bioactive Compounds As Potential Inhibitors of Oral Cancer. Future Science OA. 2022; 8(3).

[12] Natarajan PM, Umapathy VR. Role of transcriptomics in the study of oral cancer. Frontiers in Oral Health. 2025; 6:1524364.

[13] Vidhyarekha U, Natarajan PM, Bhuminathan S, Sabarinathan J, Suba R, Vijayalakshmi P. Role of artificial intelligence in Oral Cancer. Advances in Public Health. 2024. 2024: 3664408.

[14] Ganesan A, Kumar NG, Natarajan PM, Gauthaman J. Automated classification of elongated styloid processes using deep learning models-an artificial intelligence diagnostics. Frontiers in Oral Health. 2025; 5: 1424840.

[15] Umapathy VR, Natarajan PM, Swamikannu B. Regenerative Strategies in Dentistry: Harnessing Stem Cells, Biomaterials and Bioactive Materials for Tissue Repair. Biomolecules. 2025; 15: 546.

[16] Natarajan PM. Dental Bioinformnatics-Current Scope and Future perspectives. Research Journal of Pharmacy and Technology. 2022;15(5):2351-6.

[17] Ganesan A, Kumar NG, Natarajan PM. Solanum trilobatum leaf extract-derived silver nanoparticles downregulate the PI3K/AKT/mTOR signaling pathway and attenuate oral squamous cell carcinoma cell proliferation. Journal of Herbmed Pharmacology. 2024; 13(2): 300-307.

[18] Perumal MKK, Renuka RR, Subbiah SK, Natarajan PM. Artificial intelligence-driven clinical decision support systems for early detection and precision therapy in oral cancer: a mini review. Frontiers in Oral Health. 2025; 6: 1592428.

[19] Ramesh E, Ganesan A, Lakshmi KC, Natarajan PM. Artificial intelligence-based diagnosis of oral leukoplakia using deep convolutional neural networks Xception and MobileNet-v2. Frontiers in Oral Health. 2025; 6: 1414524.

[20] Ganesan A, Kumar NG, Natarajan PM. Anticancer activity of silver nanoparticles synthesized from aqueous leaf extract of Solanum trilobatum (Purple fruit pea eggplant) on human oral cancer cells. Journal of Herbmed Pharmacololgy. 2024; 13(2): 260-268.

[21] Jayaraman S, Prasad M, Natarajan SR, Krishnamoorthy R, Alshuniaber MA, Gatasheh MK, Veeraraghavan VP, Rajagopal P, Palanisamy CP. Molecular mechanisms underlying the effects of beta-sitosterol on TGF-β1/Nrf2/SIRT1/p53-mediated signaling in the kidney of a high-fat diet and sucrose-induced type-2 diabetic rat. Chemico-Biological Interactions. 2025; 411: 111443.
[22] Huang Y, Guo H, Liu Y, Jin W, Palanisamy CP, Pei J, Oz F, El-Aty AMA. Effects of Natural Polysaccharides on the Gut Microbiota Related to Human Metabolic Health. Molecular Nutrition & Food Research. 2025; e202400792.
[23] Prabhakaran P, Palanisamy CP, Shanmugam A, Damodharan P, Swaminathan H, Devaraj D, Ahalliya RM, Kanniappan GV. Isolation, structural characterization, and molecular docking studies on the bioactive compound from n-Hexane extract of Emilia sonchifolia (L.) DC against the pancreatic cancer target Aurora 2 Kinase. Journal of Complementary and Integrative Medicine. 2024; 22(1): 0290.
[24] Jiang H, Kumarasamy RV, Pei J, Raju K, Kanniappan GV, Palanisamy CP. Integrating engineered nanomaterials with extracellular vesicles: Advancing targeted drug delivery and biomedical applications. Frontiers in Nanotechnology. 2024; 6: 1513683.
[25] Guo H, Liu Y, Wan T, Song D, Palanisamy CP, Geng J, Pei J, Özmen S, El-Aty AMA. Toward personalized cancer management: Role of precision nutrition–diet interventions. Journal of Functional Foods. 2024; 123: 106584.
[26] Natarajan SR, Krishnamoorthy R, Alshuniaber MA, Al-Anazi KM, Farah MA, Rajagopal P, Palanisamy CP, Veeraraghavan VP, Jayaraman S. Identification of FOXM1 as a novel protein biomarker and therapeutic target for colorectal cancer progression: Evidence from immune infiltration and bioinformatic analyses. International Journal of Biological Macromolecules. 282 (Part 4): 137201.
[27] Rajendran MS, Jayaraman S, Khan JM, Jasmine S, Prabhakaran RK, Raju MV, Chandrasekaran MK, Ahalliya RM, Kannappan P, Palanisamy CP, Kanniappan GV. Investigating the colon toxicity and carcinogenic role of monosodium glutamate compared with Dimethylhydrazine in male Wistar rats: Exploring the link to childhood colon cancer risk. Journal of King Saud University - Science. 2024; 36(11): 103507.
[28] Kumarasamy RV, Natarajan P, Umapathy VR, Roy JR, Rab SO, Saeed M, Panagal M, Mironescu M, Srinivasan GP, Palanisamy CP. Clinical Applications and Therapeutic Potentials of Advanced Nanoparticles: A Comprehensive Review on Completed Human Clinical Trials. Frontiers in Nanotechnology. 2024; 6:1479993.
[29] Jin W, Pei JJ, Roy JR, Jayaraman S, Ahalliya RM, Kanniappan GV, Mironescu M, Palanisamy CP. Comprehensive review on single-cell RNA sequencing: A new frontier in Alzheimer's disease research. Ageing Research Reviews. 2024; 274: 102454.
[30] Pei J, Palanisamy CP, Jayaraman S, Natarajan PM, Umapathy VR, Roy JR, Panagal M, Jayaraman S. Curcumin-loaded polymeric nanomaterials as a novel therapeutic strategy for Alzheimer's disease: A comprehensive review. Ageing Research Reviews. 2024; 99: 102393.
[31] Natarajan PM, Swamikannu B, Sivaraman NM, Stylin AGSQ. Prevention of Oral Cancer: A Comprehensive Guide. Journal of Pharmacy and Bioallied Sciences. 2024; 16(5): S4239-S4241.
[32] Umapathy V, Dhanavel A, Kesavan R, Natarajan PM, Bhuminathan S, Vijayalakshmi P. Anticancer Potential of the Principal Constituent of Piper nigrum, Piperine: A Comprehensive Review. Cureus. 2024; 16(2): e54425.
[33] Umapathy VR, Swamikannu B, Natarajan PM, Devi R, Nandini MS, Vimalarani, Vijayalakshmi P. In Silico Molecular Docking of Ocimum sanctum Phytochemicals: Targeting Key Biomarkers in Oral Cancer. Journal of Pharmacy and Bioallied Sciences. 2024; 16(5): S4792-S4799.
[34] Natarajan PM, Bhuminathan S, Rajan R, Bindu K, Loganathan K, Veerakumar R. The Crucial Role of Smoking Cessation in Preventing Oral Cancer. Journal of Pharmacy and Bioallied Sciences. 2024; 16(5): S4245-S4247.
[35] Swamikannu B, Umapathy VR, Natarajan PM, Nandini MS, Stylin AGSQ, Vimalarani V, Rajinikanth S. Unlocking the Therapeutic Benefits of Artemisia Annua: A Comprehensive Overview of its Medicinal Properties. Journal of Pharmacy and Bioallied Sciences. 2024; 16(5): S4248-S4253.
[36] Natarajan PM. Computational Studies on Recent Congeners of Fluoroquinolones and Nitroimidazoles for Their Use in Periodontal Therapy. Journal of Pharmacy and Bioallied Sciences. 2024; 16(5): S4731-S4740.
[37] Yadalam PK, Arumuganainar D, Natarajan PM, Ardila CM. Artificial intelligence-powered prediction of AIM-2 inflammasome sequences using transformers and graph attention networks in periodontal inflammation. Scientific Reports. 2025; 15: 8733.
[38] Yadalam PK, Chatterjee S, Natarajan PM, Ardila CM. Comparison of light gradient boosting and logistic r egression for interactomic hub genes in Porphyromonas gingivalis and Fusobacterium nucleatum-induced perio dontitis with Alzheimer's disease. Frontiers in Oral Health. 2025; 6:1463458.
[39] Natarajan PM, Bhuminathan S, Leela B, Bindu K, Loganathan K, Ramachandran V. Smoking and its Role in Oral Cancer. Journal of Pharmacy and Bioallied Sciences 16(5): S4242-S4244.
[40] Yadalam PK, Natarajan PM, Ardila CM. Variational graph autoencoder for reconstructed transcriptomic data associated with NLRP3 mediated pyroptosis in periodontitis. Scientific Reports. 2025; 15: 1962.
[41] Pei JJ, Perumal NC, Meng P, Long Q, Palanisamy CP*. AI-assisted FTIR spectroscopic profiling of exosomes: Emerging frontiers in early detection of Alzheimer’s disease. Ageing Research Reviews. 2026; 103311.
[42] Raja FSD, Abraham L, Rangasamy K, Saikia K, Rathankumar AK, Mironescu M, Mironescu I, Palanisamy CP, Kanniappan GV. Next-Generation Microbiome Therapeutics: Psychobiotics and Fecal Microbiota

Transplants (FMT) for Mental Health Treatment. Frontiers in Cellular and Infection Microbiology. 2026; 16: 1719357.
[43] Subramani K, Srinivasan S, Shanmugam P, Palanisamy CP, Sonsudin F, Poompradub S. Sustainable phytochemical mediated-ZnO nanoparticles derived from Crescentia cujete for toxicological evaluation and multifunctional environmental applications. Environmental Nanotechnology, Monitoring & Management. 2026; 26: 101180.
[44] Kunamalla RP, Panagal M, Palanisamy CP. Green-engineered multiscale starch/PVA nanofibrous scaffolds embedded with CuO nanoparticles from Sargassum ilicifolium for potent antimicrobial performance. Genetics and Molecular Research. 2026; 25(13s): 1-9.
[45] Dharmaprakash S, Gunasekaran VP, Sivaramakrishnan R, Kanniappan GV, Jayaraman S, Mironescu M, Rajabathar JR, Mironescu ID, Palanisamy CP. Marine macroalgae-mediated ultrasonic-assisted green synthesis of CuO nanoparticles embedded in starch/PVA electrospun nanoscaffolds for in vitro α-amylase and α-glucosidase inhibitory activity. Scientific Reports. 2026; 16: 26243.
[46] Surendran N, Chandrasekaran G, Raju MV, Chandrasekaran MK, Ahalliya RM, Palanisamy CP, Kanniappan GV, Arcot R, Alharbi NS, Thiruvengadam M. Anti-inflammatory potential of ethanolic extract of Maranta arundinacea L.: Insights from COX-2 modulation and oxidative stress analysis. South African Journal of Botany. 2026; 195: 142-151.
[47] Pei J, Senthilkumar MV, Hessini K, Subramaniyam S, Sivaramakrishnan R, Kanniappan GV, Jayaraman S, Palanisamy CP. Green fabrication of starch/PVA/CuO nanoscaffolds using marine macroalgae extract for enhanced anti-inflammatory activity. Sustainable Chemistry and Pharmacy. 2026; 51: 102397.
[48] Balasubramanian V, Loganathan L, Muthuswamy K, Viswanathan TM, Raju MV, Chandrasekaran MK, Ahalliya RM, Poorasamy J, Palanisamy CP, Dominic S, Kanniappan GV. Anticancer therapeutic efficacy of PEGylated β-galactosidase from Aspergillus terreus in DMBA-induced breast cancer: Toxicological, molecular and histopathological evaluation in Wistar rats. International Journal of Biological Macromolecules. 2026; 360: 151856.
[49] Jayaraman S, Eswaran A, Rajagopal P, Palanisamy CP, Veerakumar P, Veeraraghavan VP, Sirasanagandla SR. Neuroendocrine-associated epigenetic factors in cellular senescence: mechanisms and therapeutic implications. Biogerontology. 2026; 27(2): 64.
[50] Ponnusamy B, Rajagopal P, Palanisamy CP, Veeraraghavan VP, Jayaraman S. Mechanistic Exploration of the anticancer activity of Justicia adhatoda Plant Leaf Ethanolic Extract against Colon Cancer Cells: An in silico and in vitro Approach. Asian Pacific Journal of Cancer Prevention. 2026; 27(3): 1069-1080.
[51] Pei J, Saran VS, Sivaramakrishnan R, Kanniappan GV, Pandurangan V, Jayaraman S, Dhayalan VK, Mironescu M, Mironescu ID, Palanisamy CP. Ultrasonic-assisted, Sargassum ilicifolium (brown marine macroalgae)-mediated biogenic synthesis of CuO nanoparticles incorporated in starch/PVA electrospun nanoscaffolds: In vitro safety and antioxidant efficacy assessment. Bioorganic Chemistry. 2026; 173: 109679.
[52] Raj MAPA, Subramaniyam S, Kanniappan GV, Jayaraman S, Palanisamy CP. Sustainable fabrication of starch/PVA/CuO electrospun nanoscaffolds from Turbinaria ornata (marine macroalgae) extract: Physicochemical characterization and antidiabetic evaluation. Kuwait Journal of Science. 2026; 53(2): 100545.
[53] Pei J, Ganesh NS, Subramaniyam S, Sivaramakrishnan R, Kanniappan GV, Jayaraman S, Palanisamy CP. Sustainable fabrication of starch/PVA/CuO electrospun nanoscaffolds from Padina tetrastromatica (Brown macroalgae) extract: Physicochemical characterization and antidiabetic assessment. Sustainable Chemistry One World. 2026; 9: 100195.
[54] Sakthiraj A, Sivaramakrishnan R, Subramaniyam S, Kanniappan GV, Pandurangan V, Jayaraman S, Dhayalan VK, Mironescu M, Mironescu ID, Palanisamy CP. Starch/PVA electrospun nanoscaffolds loaded with ultrasonic-assisted green-synthesis of CuO nanoparticles from marine macroalgae (Gracilaria corticata) extract: Cytotoxicity and antioxidant analysis. Chemical Physics Impact. 2026; 12: 101018.
[55] Raju M, Chandrasekaran MK, Loganathan L, Ahalliya RM, Mironescu M, Mironescu ID, Palanisamy CP, Kanniappan GV. Lipid remodeling and ferroptosis in phosphatidylcholine-mediated tumor–stroma crosstalk. Frontiers in Molecular Biosciences. 2026; 13: 1742305.
[56] Kunamalla R, Panagal M, Palanisamy CP. Biogenic synthesis and fabrication of starch/PVA/CuO electrospun nanoscaffolds from Sargassum ilicifolium (brown marine macroalgae) extract for anticancer activity on HT-29 and MCF-7 cancer cells. Biocatalysis and Agricultural Biotechnology. 2026; 72: 103923.
[57] Pei J, Govindaraj H, Sivaramakrishnan R, Kanniappan GV, Pandurangan V, Dhayalan VK, Mironescu M, Mironescu ID, Jayaraman S, Palanisamy PC. Sustainable fabrication of biopolymer-based (starch/PVA) nanoscaffolds loaded with green-synthesized CuO nanoparticles from Sargassum wightii (marine macroalgae): Cytocompatibility and antioxidant activity. Biomaterials Advances. 2026; 182: 214660.
[58] Pei J, Perumal NC, Meng P, Long Q, Palanisamy CP. Extracellular vesicle-based biosensors for Alzheimer's disease: A new frontier in precision diagnostics. Ageing Research Reviews. 2026; 113: 102904.
[59] Shree P, Sivaramakrishnan R, Kanniappan GV, Pandurangan V, Jayaraman S, Dhayalan VK, Mironescu M, Mironescu ID, Palanisamy CP. Antioxidant and biocompatible CuO-starch/PVA nanoscaffolds via ultrasonic green synthesis using Turbinaria conoides (brown marine macroalgae). Medicine in Drug Discovery. 2025; 28: 100238.
[60] Gong J, Lin J, Guan T, Pei J, Palanisamy CP, El-AtyFrom AMA. selenium tolerance to nanoplastic antagonism: Comprehensive characterization of L. casei SNUT1 and its extracellular vesicle–nanoselenium

complex. Food Bioscience. 2025; 74: 107749.
[61] Poochi SP, Sundarraj R, Raju MV, Chandrasekaran MK, Ahalliya RM, Palanisamy CP, Kanniappan GV, Kondapavuluri BK, Thiruvengadam M. Harnessing Nature: Computational and Experimental Insights Into *Ipomoea obscura* Metabolites for Bladder Cancer Therapy. Chemistry and Biodiversity. 2025; 0: e00909.
[62] Pei J, Palanisamy CP, Jayaraman S, Natarajan PM, Umapathy VR, Roy JR, Thalamati D, Ahalliya RM, Kanniappan GV, Mironescu M. A comprehensive review on starch-based Sustainable Edible Films Loaded with Bioactive Components for Food Packaging. International Journal of Biological macromolecules. 2024; 274 (Part-1): 133332.
[63] Palanisamy CP, poompradub S, Sansanaphongpricha K, Subramani K, Sonsudin F. Increased expression levels of PDGF and VEGF magnify the wound healing potential facilitated by biogenic synthesis of silver nanoparticles. Nano-Structures & Nano-Objects. 2024; 39: 101236.
[64] Pei J, Palanisamy CP, Jayaraman S, Natarajan PM, Umapathy VR, Roy JR, Thalamati D, Ahalliya RM, Kanniappan GV, Mironescu M. Proteomics Profiling of Extracellular Vesicle for Identification of Potential Biomarkers in Alzheimer's Disease: A Comprehensive Review. Ageing Research Reviews. 2024; 99: 102359.
[65] Xi J, Wang T, Xian P, Liu X, Du M, Yang H, Palanisamy CP, Lin W, Long Q. Proteomic insights uncover enhanced neurotherapeutic potential in conditioned mesenchymal stem cell-derived extracellular vesicles. Extracellular Vesicle. 2024; 3: 100037.
[66] Pei J, Natarajan PM, Umapathy VR, Swamikannu B, Sivaraman NM, Krishnasamy L, Palanisamy CP. Advancements in the synthesis and functionalization of zinc oxide-based nanomaterials for enhanced oral cancer therapy. Molecules. 2024; 29(11): 2706.
[67] Gatasheh MK, Natarajan SR, Krishnamoorthy R, Alsulami TS, Rajagopal P, Palanisamy CP, Veeraraghavan VP, Jayaraman S. Molecular analysis to identify novel potential biomarkers as drug targets in colorectal cancer therapy: an integrated bioinformatics analysis. Molecular and Cellular Oncology. 2024; 11(1): 2326699.
[68] Pei J, Yan Y, Jayaraman S, Rajagopal P, Natarajan PM, Umapathy VR, Gopathy S, Roy JR, Sadagopan CS, Thalamati D, Palanisamy CP, Mironescu M. A review on advancements in the application of starch-based nanomaterials in biomedicine: Precision drug delivery and cancer therapy. International Journal of Biological Macromolecules. 2024; 130746.
[69] Pei JJ, Yan Y, Palanisamy CP, Jayaraman S, Natarajan PM, Umapathy VR, Gopathy S, Roy JR, Sadagopan JC, Thalamati D, Mironescu M. Materials-based drug delivery approaches: Recent advances and future perspectives. Green Processing and Synthesis. 2024; 13: 20230094.
[70] Pei JJ, Deng W, Liu Y, Guo Y, Chen J, Abdu H, Khan MR, Palanisamy CP, El-Aty AM. A Comprehensive Review of Cornus officinalis: Health Benefits, Phytochemistry, and Pharmacological Effects for Functional Drug and Food Development. Frontiers in Nutrition. 2023; 10: 1309963.
[71] Alugoju P, Palanisamy CP, Anthikapalli NVA, Jayaraman S, Prasanskulab A, Chuchawankul S, Dyavaiah M, Tencomnao T. Exploring the anti-aging potential of natural products and plant extracts in budding yeast Saccharomyces cerevisiae: A review. F1000Research. 2023; 12: 1265.
[72] Lavanya M, Krishnamoorthy R, Alshuniaber MA, Manoharadas S, Palanisamy CP, Veeraraghavan VP, Jayaraman S, Rajagopal P, Padmini R. Formulation, characterization and evaluation of gelatin-syringic acid/zinc oxide nanocomposite for its effective anticancer, antioxidant and anti-inflammatory activities. Journal of King Saud University-Science. 2023; 35: 102909.
[73] Palanisamy CP, Poompradub S, Sansanaphongpricha K, Jayaraman S, Subramani K, Sonsudin F. Biosynthesis of silver nanoparticles (AgNPs) using ethanolic extract of Nigella sativa (L.) seeds promotes wound healing via PDGF and VEGF signalling pathways activation. Biocatalysis and Agricultural Biotechnology. 2023; 54: 102970.
[74] Prasad M, Jayaraman S, Natarajan SR, Veeraraghavan VP, Krishnamoorthy R, Gatasheh MK, Palanisamy CP, Elrobh M. Piperine modulates IR/Akt/GLUT4 pathways to mitigate insulin resistance: Evidence from animal and computational studies. International Journal of Biological Macromolecules. 2023; 253: 127242.